Available online at www.sciencedirect.com
SCIENCE DIRECT®
Journal of Sound and Vibration 272 (2004) 513–537
JOURNAL OF SOUND AND VIBRATION
www.elsevier.com/locate/jsvi

Cancellation techniques in underwater scattering of acoustic signals

C.L. Scandrett[a], Y.S. Shin[a], K.C. Hung[b,*], M.S. Khan[b], C.C. Lilian[c]

[a] *Naval Postgraduate School, Monterey, CA, USA*
[b] *Institute of High Performance Computing, 1 Science Park Road, #01-01 The Capricorn, Singapore Science Park II, Singapore 117528, Singapore*
[c] *DSO National Laboratories, 20 Science Park Drive, Singapore 118230, Singapore*

Received 5 November 2001; accepted 28 March 2003

Abstract

Advanced materials made of a combination of viscoelastic coating and piezoelectric substances are fast emerging as important acoustics materials that can be used to reduce or eliminate scattered acoustic signals of submerged structures. In this paper, we considered the underlying principles that govern the acoustic performance of viscoelastic and piezoelectric materials. Analytical treatments such as the invariant embedding techniques, potential method, Floquet theory and asymptotics approximation, are employed to derive the mathematical model for predicting the acoustics performance of viscoelastic and piezoelectric materials. Numerical implementations in finite difference methods coupled with boundary integral formulation, and commercial finite elements code, such as ANSYS, are demonstrated for some practical configurations. Results for a few representative canonical examples of the problem, which include two-dimensional acoustic scattering from a fluid-loaded plate embedded with viscoelastic material or piezoelectric elements served as useful benchmarks for future works in this direction.

1. Introduction

The Office of Naval Research has identified 5 areas related to ship signature that are receiving a great deal of attention [1]. The five areas consist of underwater acoustic, infrared, radar cross-section, electromagnetic compatibility, and underwater electromagnetic. Of these, the underwater acoustic signature appears to be the most "exploitable" feature of a ship's signature. It is

*Corresponding author. Institute of High Performance Computing, 1 Science Park Drive, #01-01 The Capricorn, Singapore Science Park II, Singapore 117528, Singapore.
E-mail address: hungkc@ihpc.a-star.edu.sg (K.C. Hung).

0022-460X/03/$ - see front matter
doi:10.1016/S0022-460X(03)00381-X

exploitable in either a passive mode, where transducers listen for radiated noise from a ship, or in an active mode, where a ship is insonified by an acoustic field that generates a scattered acoustic response. Sources of radiated acoustic noise come primarily from internal structures of a ship such as propulsion engines or from external fluid flow over the hull and/or appendages of the ship. Naval ships are subjected to acoustic interrogation (either passive or active) by increasingly sophisticated underwater transducers and transducer arrays. Hence, technologies that may enhance a ship's "stealth" capabilities are of interest to many navies.

Passive treatment in reduction of acoustic radiation or scattering involves the use of sophisticated materials that act as dampers of acoustic/structural wave propagation (for example viscoelastic layers) [2]. Various authors [3–5] have studied the effectiveness of compliant coatings in reducing reflections from and radiation by submerged structures. Mathematical and numerical models to determine the effective impedance of such layers have also been derived [6–8].

Active treatment of acoustic signals, on the other hand, requires the use of piezoelectric substances such as PZT and polyvinylidene fluoride (PVDF) that have the ability to actively alter their acoustic properties by the introduction of electric fields or voltage potentials. This unique property of the piezoelectric substances can be exploited to generate acoustic disturbances in the manufacturing of underwater transducers [9], or for the purpose of suppressing unwanted reflections or radiation from underwater structures [10–15]. The Varadan's were involved in four of the cited works. In particular, Ref. [10] evaluated electrical circuit models of a bilaminate fluid-loaded plate, while Refs. [13,14], are concerned with finite element modelling of fluid-loaded piezoelectric, and piezoelectric embedded plates. Ref. [12] reports on experiments involving one-dimensional (1-D) water-filled pulse tubes. The work of Braga [11] provides much of the underlying principles of the physics and related mathematical considerations in this area of wave propagation. In his treatment, analytical forms for reflection coefficients generated by scattering from a layered material are found by invariant imbedding techniques [16]. Aside from the references just cited, other publications in the area of material design for signal reduction are very limited.

The advances in material science and signal processing techniques have led to the emerging of new acoustic materials that combine the passive coating with active piezoelectric substances for broadband noise cancellation. Mathematical and numerical models that are capable of simulating the underlying physics of these hybrid acoustic materials will be of great interest to researchers in the area of underwater acoustics. This paper is concerned with the formulation of a mathematical framework for the acoustics analysis of advanced materials. The modelling of viscoelastic layer and piezoelectric substances is based on the invariant embedding technique and the potential method. Solutions of representative canonical problems in acoustic radiation and scattering are presented to illustrate the approach. Finally, application examples are given to show the effect of piezoelectric substances for acoustic signal reduction. The mathematical formulation and the numerical results presented in this paper will be useful to the study of broadband acoustics signal reduction using hybrid viscoelastic and piezoelectric materials.

2. Geometry's of problems considered

The geometry for the first few problems discussed is given in Fig. 1 below. There is an elastic slab of thickness t_e fluid loaded above, and in perfect welded contact to either a

vacuum backed viscoelastic (or piezoelectric) layer of thickness t_v (or t_p). The radiation problem considered here is two-dimensional (2-D), implying that the resulting fluid pressures produced by either the applied voltages across the piezoelectric layer or applied normal stress on the underside of the viscoelastic layer are planar. The material properties of the media are given in Table 1.

For PZT4, there are several parameters that characterize the anisotropic material. In particular, the elastic (stiffness) moduli are: $c_{11} = 1.39 \times 10^{11}$ Pa, $c_{13} = 7.784 \times 10^{10}$ Pa, $c_{33} = 1.1541 \times 10^{11}$ Pa, $c_{44} = 2.564 \times 10^{10}$ Pa; the dielectric constants are: $\varepsilon_1 = 730\varepsilon_0$, $\varepsilon_3 = 635\varepsilon_0$, where $\varepsilon_0 = 8.85 \times 10^{-12}$ F/m is the free space dielectric constant; and the piezoelectric constants are: $e_{15} = 12.718\,\mathrm{C/m^2}$, $e_{31} = -5.203\,\mathrm{C/m^2}$, $e_{33} = 15.08\,\mathrm{C/m^2}$. These values for PZT4 were taken from the ANSYS library [17], while those for the viscoelastic material listed in the table, are valid at a frequency of 1 kHz, and are taken from a monogram by Nashif and Jones [18]. A second viscoelastic material *with* frequency-dependent material parameters was taken from Ref. [19], where it was characterized as a soft polymer. Its material parameters at frequency f are given by $\log_{10}(\|\mu\|) = 5.93978 + 0.26618\log_{10}(f) - 0.03613 \times (\log_{10}(f))^2 + 0.0041(\log_{10}(f))^3$; $\delta_\mu = 0.05251 + 0.19374\,log_{10}(f) - 0.06209(\log_{10}(f))^2 + 0.00819(\log_{10}(f))^3$; bulk modulus $= 3 \times 10^9 \times (1 - \delta_\mu i)$; shear modulus $= ||\mu|| \times (1 - \delta_\mu i)$; density $= 935\,\mathrm{kg/m^3}$.

The canonical problems of scattering and radiation from a *baffled*, bilaminate are also considered in this study. The geometry is similar to the infinite case, except that the fluid structure interaction is truncated by the addition of a baffle which serves as boundary of the numerical domain. A geometrical set-up for this problem is given in Fig. 2 below.

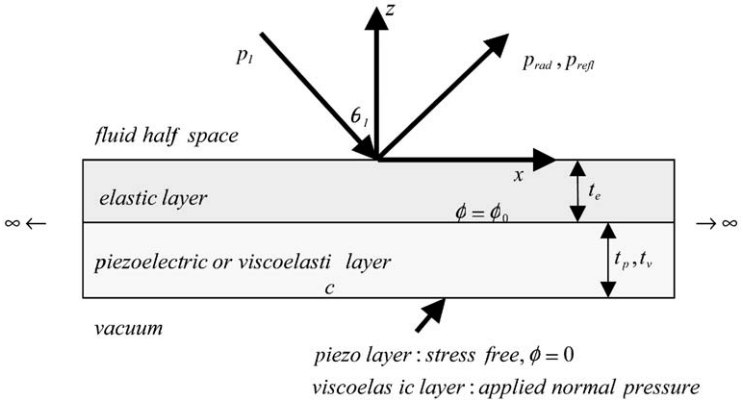

Fig. 1. Schematic of acoustics radiation and reflection from infinite bilaminates.

Table 1
Properties of media and materials used in the present study

Media	Density (kg/m^3)	Young's modulus (Pa)	Shear modulus (Pa)
Water	$\rho_f = 1000$	2.25×10^9 (Bulk)	0
Elastic	$\rho_e = 7850$	2.07×10^{11}	8.10×10^{10}
Viscoelastic (FEM)	$\rho_v = 909$	$8.22 \times 10^6(1-i)$	$2.758 \times 10^6(1-i)$

3. Mathematical framework

The governing equations used in this paper for the elastic and viscoelastic materials can be found in standard texts on elastic wave propagation [20]. The equations are:

$$\text{Stress}: \; S_{ij} = \frac{1}{2}\left(\frac{\partial u_i}{\partial x_j} + \frac{\partial u_j}{\partial x_i}\right) = \frac{1}{2}(u_{i,j} + u_{j,i}) \quad i,j = 1,2,3, \tag{1}$$

$$\text{Stress/strain relation}: \; T_{ij} = c_{ijkl} S_{kl} \quad i,j,k,l = 1,2,3, \tag{2}$$

$$\text{Eq. of motion}: \; \frac{\partial T_{ij}}{\partial x_j} + F_i = \rho \frac{\partial^2 u_i}{\partial t^2} \quad F_i \text{ body forces}, \tag{3}$$

where u_i, S_{ij}, T_{ij}, and c_{ijkl} are the elastic displacements, stress, strain, and stiffness constants of the elastic material.

For a piezoelectric material, coupling between the elastic and electromagnetic effects is modelled by the piezoelectric coupling equations

$$D_i = \varepsilon_{ij}^S E_j + e_{iJ} S_J, \quad T_I = -e_{Ij} E_j + c_{IJ}^E S_J, \tag{4}$$

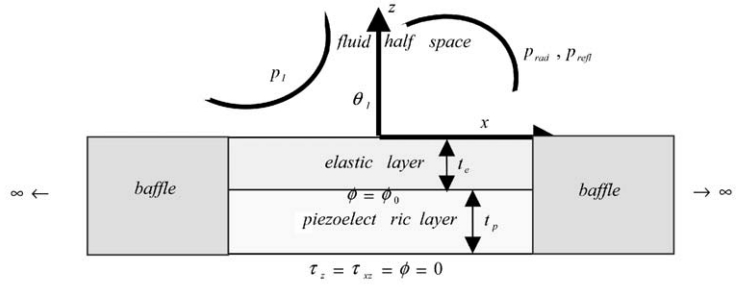

(a)

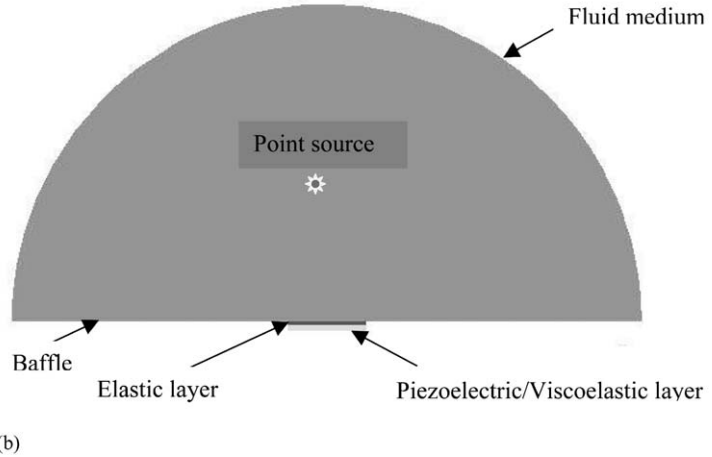

(b)

Fig. 2. Radiation and reflection from a baffled elastic/piezo bilaminate (a) schematic of the baffled bilaminated plate, (b) boundary of fluid domain and the location of a point source.

in which D_i, E_j, e_{iJ}, and ε_{ij}^s are the displacement current, electric field, piezoelectric coupling constants, and the dielectric matrix of the piezoelectric material. Note that abbreviated notation is used to represent the stress and strain fields as well as the stiffness and piezoelectric constant matrices. The convention used is an IEEE standard [21], but differs slightly from that used in the ANSYS finite element code [17].

Because of the huge difference in wave speeds for elastic and electromagnetic waves, a quasi-static approximation is used which neglects the rotational portion of the electromagnetic field in favor of the solenoid. With this approximation, the coupled equations of motion for a piezoelectric material are:

$$\frac{\partial}{\partial x_i}\left[\varepsilon_{ij}^S \frac{\partial \Phi}{\partial x_j}\right] = \frac{\partial}{\partial x_i}[e_{iJ}\nabla_{Jk}u_k],$$
$$\nabla_{iJ}c_{JK}^E \nabla_{Km}u_m + \nabla_{iJ}e_{Jk}\frac{\partial^2 \Phi}{\partial x_k^2} = \rho \frac{\partial^2 u_i}{\partial t^2}, \tag{5}$$

where Φ is the electrostatic potential in the piezoelectric. An implicit assumption is made that no free charge exists in the material. The differential operator in the above equation again uses the abbreviated index notation mentioned previously.

For the special case of 2-D plane strain involving isotropic, homogeneous elastic media and piezoelectric materials belonging to the hexagonal symmetry class of crystals poled along the z-axis (PZT4 and PZT5 are of this type), the governing equations of motion can be written:

For the piezoelectric substance:

$$c_{11}\frac{\partial^2 u_p}{\partial x^2} + (c_{13}+c_{44})\frac{\partial^2 w_p}{\partial x \partial z} + c_{44}\frac{\partial^2 u_p}{\partial z^2} - \rho_p \frac{\partial^2 u_p}{\partial t^2} = -(e_{31}+e_{15})\frac{\partial^2 \Phi}{\partial x \partial z},$$
$$c_{44}\frac{\partial^2 w_p}{\partial x^2} + (c_{13}+c_{44})\frac{\partial^2 u_p}{\partial x \partial z} + c_{33}\frac{\partial^2 w_p}{\partial z^2} - \rho_p \frac{\partial^2 w_p}{\partial t^2} = -e_{33}\frac{\partial^2 \Phi}{\partial z^2} - e_{15}\frac{\partial^2 \Phi}{\partial x^2},$$
$$\varepsilon_1 \frac{\partial^2 \Phi}{\partial x^2} + \varepsilon_3 \frac{\partial^2 \Phi}{\partial z^2} = (e_{31}+e_{15})\frac{\partial^2 u_p}{\partial x \partial z} + e_{15}\frac{\partial^2 w_p}{\partial x^2} + e_{33}\frac{\partial^2 w_p}{\partial z^2}. \tag{6}$$

For the elastic or viscoelastic substance:

$$(\lambda+2\mu)\frac{\partial^2 u_e}{\partial x^2} + (\lambda+\mu)\frac{\partial^2 w_e}{\partial x\,\partial z} + \mu\frac{\partial^2 u_e}{\partial z^2} - \rho_e \frac{\partial^2 u_e}{\partial t^2} = 0,$$
$$\mu\frac{\partial^2 w_e}{\partial x^2} + (\lambda+\mu)\frac{\partial^2 u_e}{\partial x\,\partial z} + (\lambda+2\mu)\frac{\partial^2 w_e}{\partial z^2} - \rho_e \frac{\partial^2 w_e}{\partial t^2} = 0, \tag{7}$$

and for the fluid medium the simple acoustic wave equation:

$$\frac{\partial^2 p}{\partial x^2} + \frac{\partial^2 p}{\partial z^2} - \frac{1}{c_f^2}\frac{\partial^2 p}{\partial t^2} = 0. \tag{8}$$

In the above system of equations, "e" subscripts refer to elastic displacements, while "p" subscripts refer to the piezoelectric material, u and w are the displacements in the x and z directions, respectively, λ and μ are the Lame' constants for the elastic material, ρ_e, ρ_p, and ρ_f are the elastic, piezoelectric, and fluid material densities, and p is the pressure in the fluid which has an acoustic wave speed of c_f.

At the interface between the elastic and fluid media, continuity of both the normal strain and normal velocity is applied, while the shear stress must vanishes leading to the boundary conditions

$$(\lambda + 2\mu)\frac{\partial w_e}{\partial z} + \lambda\frac{\partial u_e}{\partial x} = -p, \quad \mu\left(\frac{\partial w_e}{\partial x} + \frac{\partial u_e}{\partial z}\right) = 0, \quad \frac{\partial p}{\partial z} = -\rho_f \frac{\partial^2 w_e}{\partial t^2}. \tag{9}$$

At the elastic/piezoelectric boundary one has continuity of stress and displacement leading to the conditions

$$\begin{aligned} &u_e = u_p, \quad w_e = w_p, \\ &(\lambda + 2\mu)\frac{\partial w_e}{\partial z} + \lambda\frac{\partial u_e}{\partial x} = e_{33}\frac{\partial \Phi}{\partial z} + c_{13}\frac{\partial u_p}{\partial x} + c_{33}\frac{\partial w_p}{\partial z}, \\ &\mu\left(\frac{\partial w_e}{\partial x} + \frac{\partial u_e}{\partial z}\right) = e_{15}\frac{\partial \Phi}{\partial x} + c_{44}\left(\frac{\partial u_p}{\partial z} + \frac{\partial w_p}{\partial x}\right). \end{aligned} \tag{10}$$

For the interface between an elastic and viscoelastic material, the conditions listed above on the left side of the equations must be matched by equivalent terms using the material properties and displacements of the viscoelastic substance when two materials are in perfect contact.

The boundary condition for the electric potential function at the piezoelectric/elastic interface is given by

$$\Phi = \Phi_0.$$

At the bottom (free) surface of the piezoelectric layer, the potential is grounded ($\Phi = 0$), and the normal and tangential stress components must vanish leading to the equations

$$e_{33}\frac{\partial \Phi}{\partial z} + c_{13}\frac{\partial u_p}{\partial x} + c_{33}\frac{\partial w_p}{\partial z} = 0, \quad e_{15}\frac{\partial \Phi}{\partial x} + c_{44}\left(\frac{\partial u_p}{\partial z} + \frac{\partial w_p}{\partial x}\right) = 0, \quad \Phi = 0. \tag{11}$$

All problems considered assume a time dependence given by $\exp(-i\omega t)$, for which time domain results could be found using fast Fourier transforms. Initial conditions for each of the problems are unnecessary since steady state solutions are sought. Radiation and/or decaying conditions are needed however to eliminate unrealistic waves such as those, which blow up as they propagate or come from infinity. At large distances from a finite scatterer the condition is referred to as the Sommerfeld radiation condition, which in two dimensions can be written

$$\frac{\partial p}{\partial r} + \frac{1}{2r}p + \frac{1}{c_f}\frac{\partial p}{\partial t} \to 0 \quad \text{as } r \to \infty. \tag{12}$$

A line source is used to perform scattering calculations from the baffled bilaminate in two dimensions. It is given by

$$p_I(x, x_0, z, z_0) = -A_P\frac{i}{4}H_0^1\left(k_f\sqrt{(x - x_0)^2 + (z - z_0)^2}\right), \tag{13}$$

in which the co-ordinates of the line source are $x = x_0$, $z = z_0$, and the amplitude A_P (in Pa) of the incident pressure is related to the source strength of the point source Q by the relationship

$$Q = \frac{A_P}{i\omega\rho_f}, \tag{14}$$

and H_0^1 is a zero order Hankel function of the first kind.

4. Analytic methods

4.1. Invariant embedding methods

It is convenient for plane wave propagation in layered media to write the system of governing partial differential equations in terms of a matrix of ordinary differential equations for a state vector which includes the depth dependent variables of stress, displacement and electric potential (see for example Ref. [22]). This is essentially the method adopted by Honein et al. in their paper on suppressing plane wave reflections from a fluid loaded piezoelectric laminate [23]. Because of the incident plane wave (or applied voltage) (x,t) time/space dependence, all field variables are written explicitly of the form

$$\vec{\Psi}(x,z,t) = \vec{\xi}(z)\mathrm{e}^{-\mathrm{i}\omega t+\mathrm{i}k_x x}, \tag{15}$$

where $k_x = k_f \sin\theta I$ is the "horizontal" wave number of the problem. The state vector for the piezoelectric layer can then be written

$$\vec{\xi}_p = \begin{bmatrix} u_p(z) \\ w_p(z) \\ D_3(z) \\ T_5(z) \\ T_3(z) \\ \Phi(z) \end{bmatrix}. \tag{16}$$

The T's in the above vector are stress components, D_3 is the electric displacement, Φ is the electric potential, and u and w are the horizontal and vertical displacements in the piezoelectric layer. With the assumed t and x dependence, the governing equations for the piezoelectric layer can be written as a matrix ordinary differential equation in the variable z which involves the so-called "Stroh" matrix A_p:

$$\frac{\mathrm{d}\vec{\xi}_p}{\mathrm{d}z} = A_p\vec{\xi}_p, \tag{17}$$

with

$$A_p = \begin{bmatrix} 0 & -\mathrm{i}k_x & 0 & 1/c_{44} & 0 & -\mathrm{i}k_x\beta_1 \\ \mathrm{i}k_x\alpha_4 & 0 & \alpha_2 & 0 & \alpha_1 & 0 \\ 0 & 0 & 0 & -\mathrm{i}k_x\beta_1 & 0 & k_x^2\beta_2 \\ -\rho_p\omega^2 + k_x^2(c_{11}+c_{13}\alpha_4+e_{31}\alpha_5) & 0 & \mathrm{i}k_x\alpha_5 & 0 & \mathrm{i}k_x\alpha_4 & 0 \\ 0 & -\rho_p\omega^2 & 0 & -\mathrm{i}k_x & 0 & 0 \\ \mathrm{i}k_x\alpha_5 & 0 & \alpha_3 & 0 & \alpha_2 & 0 \end{bmatrix},$$

$$\alpha_0 = c_{33}\varepsilon_3 + e_{33}^2, \quad \alpha_4 = -(\varepsilon_3 c_{13} + e_{33}e_{31})/\alpha_0,$$
$$\alpha_1 = \varepsilon_3/\alpha_0, \quad \alpha_5 = (c_{33}e_{31} + e_{33}c_{13})/\alpha_0,$$
$$\alpha_2 = e_{33}/\alpha_0, \quad \beta_1 = e_{15}/c_{44},$$
$$\alpha_3 = -c_{33}/\alpha_0, \quad \beta_2 = -(\varepsilon_1 + e_{15}^2/c_{44}).$$

A similar formulation for an isotropic, homogeneous, elastic or viscoelastic layer can be done leading to the state vector, differential equations, and Stroh matrix

$$\vec{\xi}_e = \begin{bmatrix} u_e(z) \\ w_e(z) \\ T_5(z) \\ T_3(z) \end{bmatrix},$$

$$\frac{\mathrm{d}\vec{\xi}_e}{\mathrm{d}z} = A_e\vec{\xi}_e, \tag{18}$$

$$A_e = \begin{bmatrix} 0 & -\mathrm{i}k_x & 1/\mu & 0 \\ -\mathrm{i}k_x\lambda/(\lambda+2\mu) & 0 & 0 & 1/(\lambda+2\mu) \\ -\rho_e\omega^2 + 4k_x^2\mu(\lambda+\mu)/(\lambda+2\mu) & 0 & 0 & -\mathrm{i}k_x\lambda/(\lambda+2\mu) \\ 0 & -\rho_e\omega^2 & -\mathrm{i}k_x & 0 \end{bmatrix}.$$

In the special case of a bilaminate, with an elastic upper layer of thickness $|z_1|$ in contact with water at $z = 0$, and a bottom piezoelectric layer of thickness $|z_2 - z_1|$ having zero voltage and zero stress along its underside, and an applied voltage of ϕ_0 at the elastic/piezo interface, the following set of interfaces conditions hold

Fluid/elastic:

$$w_e(0^-) = w(0^+) = \frac{\mathrm{i}}{\omega Z_f}(-I + R), \quad \text{where } Z_f = \frac{\rho_f c_f}{\cos\theta_I},$$
$$T_5(0) = 0, \quad T_3(0^-) = T_3(0^+) = -p(0) = -(I + R). \tag{19}$$

Elastic/piezo:

$$u_p(z_1^-) = u_e(z_1^+), \quad \text{where } z_1 = -t_e,$$
$$w_p(z_1^-) = w_e(z_1^+),$$
$$(T_p)_5(z_1^-) = (T_e)_5(z_1^+),$$
$$(T_p)_3(z_1^-) = (T_e)_3(z_1^+),$$
$$\Phi(z_1) = \Phi_0. \tag{20}$$

Piezo/free:

$$(T_p)_5(z_2) = 0, \quad \text{where } z_2 = -(t_e + t_p),$$
$$(T_p)_3(z_2) = 0,$$
$$\Phi(z_2) = 0.$$

A "surface impedance tensor" is found for the bilaminate that can be used to determine the pressure reflection and/or radiation coefficients. Steps taken to find this tensor are as follows:

- Find the eigenvalues/eigenvectors of the Stroh matrix for a given layer.
- Separate upward decaying or traveling modes from downward ones.
- Impose interface conditions at the bottom surface of the layer to determine an impedance condition at the top surface of the layer.
- Continue this process from the bottom to uppermost layer.

The resultant impedance matrix is then used at the fluid/solid interface to satisfy boundary conditions applied there that in turn determine pressure reflection and radiation coefficients.

For the particular problem considered, one starts by finding eigenvectors and eigenvalues of the piezoelectric Stroh matrix A_p. Generalized displacement and traction vectors are introduced

$$\vec{U}^P = \begin{bmatrix} u_p \\ w_p \\ D_3 \end{bmatrix} \quad \vec{V}^P = \begin{bmatrix} T_5 \\ T_3 \\ \phi \end{bmatrix},$$

and the eigenvalues are split into upward ($\lambda_i, i = 1, 2, 3$) and downward terms ($\lambda_i, i = 4, 5, 6$). (The "upward" eigenvalues are those for which $\Im m(\lambda_i) > 0$ or $\Re e(\lambda_i) < 0$ when $\Im m(\lambda_i) = 0$.)

$$\phi_1^P = \begin{bmatrix} e^{\lambda_1(z-z_2)} & 0 & 0 \\ 0 & e^{\lambda_2(z-z_2)} & 0 \\ 0 & 0 & e^{\lambda_3(z-z_2)} \end{bmatrix} \quad \text{with eigenvectors} \quad \begin{bmatrix} A_1^P \\ L_1^P \end{bmatrix}. \tag{21}$$

A_1^P and L_1^P are 3×3 matrices that include the generalized displacements and tractions of the upward eigenvectors, respectively. In a similar fashion, the downward traveling eigenvectors and eigenvalues are

$$\phi_2^P = \begin{bmatrix} e^{\lambda_4(z-z_2)} & 0 & 0 \\ 0 & e^{\lambda_5(z-z_2)} & 0 \\ 0 & 0 & e^{\lambda_6(z-z_2)} \end{bmatrix} \quad \text{with eigenvectors} \quad \begin{bmatrix} A_2^P \\ L_2^P \end{bmatrix}. \tag{22}$$

A general solution of the ordinary differential equation for the piezoelectric layer is

$$\vec{U}^P = A_1^P \phi_1^P \vec{c}_1 + A_2^P \phi_2^P \vec{c}_2, \quad \vec{V}^P = L_1^P \phi_1^P \vec{c}_1 + L_2^P \phi_2^P \vec{c}_2. \tag{23}$$

Because $\mathbf{V}^P(z_2) = 0$ at the bottom free surface, and $\boldsymbol{\phi}_i^P(z_2) = I$, one can solve for the vector $\mathbf{c}_2$ in terms of $\mathbf{c}_1 (\mathbf{c}_2 = -(L_2^P)^{-1} L_1^P \mathbf{c}_1)$, and ultimately an impedance relationship for the layer

$$\vec{V}^P(z) = G^P(z) \vec{U}^P(z), \quad z_1 > z > z_2, \tag{24}$$

where

$$Z_1^P = L_1^P (A_1^P)^{-1}, \quad Z_2^P = L_2^P (A_2^P)^{-1}, \quad R^P = -(Z_1^P)^{-1} Z_2^P, \quad M_1^P(z) = A_1^P \phi_1^P(z) (A_1^P)^{-1},$$
$$M_2^P(z) = A_2^P \phi_2^P(z) (A_2^P)^{-1}, \quad H^P(z) = M_1^P(z) R^P [M_2^P(z)]^{-1},$$
$$G^P(z) = [Z_2^P + Z_1^P H^P(z)][I + H^P(z)]^{-1}.$$

The Z_1^P and Z_2^P matrices are upward and downward wave impedances, while M_1^P and M_2^P are one-way propagator matrices for the layer.

At the interface between the piezoelectric and elastic layer ($z = z_1$), one must split off the electric field variables in order to impose continuity conditions. At $z = z_1$ the impedance relationship is split as follows

$$\vec{V}^P(z_1) = G^P(z_1)\vec{U}^P(z_1) \Rightarrow \begin{bmatrix} \vec{t}(z_1) \\ \Phi(z_1) \end{bmatrix} = \begin{bmatrix} G_1(z_1) & \vec{g}_2(z_1) \\ \vec{g}_3^T(z_1) & g_4(z_1) \end{bmatrix} \begin{bmatrix} \vec{u}(z_1) \\ D_3(z_1) \end{bmatrix}. \tag{25}$$

By applying the interface condition on the voltage potential, ($\Phi(z_1) = \Phi_0$), one can eliminate the D_3 variable from the above set of equations to obtain an impedance relationship involving only variables used in the elastic layer

$$\vec{t}^P(z_1) = g^P(z_1)\vec{u}(z_1) + \Phi_0\vec{F}^P(z_1), \tag{26}$$

with

$$g^P(z_1) = G_1(z_1) - \frac{1}{g_4(z_1)}\vec{g}_2(z_1) \quad \vec{g}_3^{\mathrm{T}}(z_1) \;\; \vec{F}^P(z_1) = \frac{1}{g_4(z_1)}\vec{g}_2(z_1).$$

Eigenvalues and eigenvectors of the elastic Stroh matrix are found and split into upward and downward parts. The displacement and traction vectors are

$$\vec{U}^E = \begin{bmatrix} u \\ w \end{bmatrix} \quad \text{and} \quad \vec{V}^E = \begin{bmatrix} T_5 \\ T_3 \end{bmatrix},$$

and the general solution to the matrix ODE for the elastic layer is

$$\vec{U}^E = A_1^E\phi_1^E\vec{c}_1 + A_2^E\phi_2^E\vec{c}_2, \quad \vec{V}^E = L_1^E\phi_1^E\vec{c}_1 + L_2^E\phi_2^E\vec{c}_2. \tag{27}$$

The four eigenvalues of the matrix ODE are associated with upward and downward traveling compressional and shear waves. The diagonal entries in the $\boldsymbol{\phi}_i^E$ matrices are of the form $\exp(\lambda_i(z - z_1))$ so that at the elastic/piezoelectric interface, ($z = z_1$), they become identity matrices. By employing the surface impedance tensor that was found for the piezoelectric layer, one can solve for $\mathbf{c}_1$ in terms of $\mathbf{c}_2$, and ultimately find the impedance matrix for the elastic layer

$$\vec{V}^E(z) = G^E(z)\vec{U}^E(z) + \Phi_0 S^E(z), \quad 0 > z > z_1, \tag{28}$$

where

$$\begin{aligned}
&Z_1^E = L_1^E(A_1^E)^{-1}, \quad Z_2^E = L_2^E(A_2^E)^{-1}, \quad R^E = -(Z_1^E - g^P(z_1))^{-1}(Z_2^E - g^P(z_1)),\\
&M_1^E(z) = A_1^E\phi_1^E(z)(A_1^E)^{-1}, \quad M_2^E(z) = A_2^E\phi_2^E(z)(A_2^E)^{-1},\\
&H^E(z) = M_1^E(z)R^E[M_2^E(z)]^{-1}, \quad G^E(z) = [Z_2^E + Z_1^E H^E(z)][I + H^E(z)]^{-1},\\
&S^E(z) = [Z_1^E - G^E(z)]M_1^E(z)[Z_1^E - g^P(z_1)]^{-1}\vec{F}^P.
\end{aligned}$$

Finally, at $z = 0$, the impedance condition is evaluated and application of the three boundary conditions is imposed. The impedance condition at $z = 0$ is written

$$\begin{bmatrix} T_5 \\ T_3 \end{bmatrix} = \begin{bmatrix} G_{11}^E & G_{12}^E \\ G_{21}^E & G_{22}^E \end{bmatrix} \begin{bmatrix} u_e \\ w_e \end{bmatrix} + \Phi_0 \begin{bmatrix} S_1 \\ S_2 \end{bmatrix}. \tag{29}$$

The boundary conditions lead to the solution for the reflection and radiation coefficients

$$R = \left[\frac{-1 + \mathrm{i}(G_{11}^E G_{22}^E - G_{12}^E G_{21}^E)/\omega Z_f G_{11}^E}{1 + \mathrm{i}(G_{11}^E G_{22}^E - G_{12}^E G_{21}^E)/\omega Z_f G_{11}^E}\right] I + \left[\frac{S_1 G_{21}^E / G_{11}^E - S_2}{1 + \mathrm{i}(G_{11}^E G_{22}^E - G_{12}^E G_{21}^E)/\omega Z_f G_{11}^E}\right] \Phi_0. \quad (30)$$

If $I = 0$, the value of R is the pressure radiation coefficient when a voltage Φ_0 is applied, while if $\Phi_0 = 0$ (the piezoelectric material is short circuited), R is the reflection amplitude caused by an incident plane wave of amplitude I. To cancel a reflected pressure wave, one must solve for the value of Φ_0 that causes $R = 0$.

The invariant embedding technique can be tested by applying a simple potential method for the case of plane wave radiation from an infinite fluid loaded layer. For the case of a single infinite layer of either elastic or viscoelastic material under the assumption of plane strain, the displacements of the solid can be written in terms of potentials [24]

$$u(x,z) = \frac{\partial \varphi}{\partial x} - \frac{\partial \psi}{\partial z} \quad w(x,z) = \frac{\partial \varphi}{\partial z} + \frac{\partial \psi}{\partial x}. \quad (31)$$

The phased time harmonic load applied to the underside of the solid layer and the resulting plane wave radiated pressure into the fluid are given by

$$F = Q\mathrm{e}^{-\mathrm{i}\omega t + \mathrm{i}k_x x}, \quad p = R\mathrm{e}^{-\mathrm{i}\omega t + \mathrm{i}k_x x + \mathrm{i}k_f z \cos\theta_I}. \quad (32)$$

Substitution of the potentials into Eq. (7), splits the coupled system into two second order wave equations for the shear and compressional potentials with solutions given by

$$\varphi = A\mathrm{e}^{\mathrm{i}k_L(x \sin\phi + z\cos\phi)} + B\mathrm{e}^{\mathrm{i}k_L(x\sin\phi - z\cos\phi)}, \quad (33)$$

$$\psi = C\mathrm{e}^{\mathrm{i}k_T(x\sin\vartheta + z\cos\vartheta)} + D\mathrm{e}^{\mathrm{i}k_T(x\sin\vartheta - z\cos\vartheta)}, \quad (34)$$

$k_L = \omega/c_L$ c_L is the compressional phase speed,

$k_T = \omega/c_T$ c_T is the shear phase speed.

As with the invariant embedding method, phases must match in the x co-ordinate (Snell's Law), and the remaining five boundary conditions can be used to determine the potential amplitudes (A, B, C, and D) and the amplitude of the radiated pressure (R). These boundary conditions are Eq. (9) applied at the fluid/solid interface (after substitution of the displacement potentials), and the first two conditions of Eq. (9) with $-p$ replaced by F, and applied at the underside of the elastic/viscoelastic layer.

5. Numerical methods

5.1. Finite element methods

The finite element analysis approach utilizes the ANSYS code. A quick review of the theoretical underpinnings of the method follows. A more elaborate treatment can be found in the ANSYS theory reference manual [25]. The electro-mechanical equilibrium equations for a piezoelectric

material behavior can be written in matrix form based on an element local co-ordinate system

$$\begin{Bmatrix} \{T\} \\ \{D\} \end{Bmatrix} = \begin{bmatrix} [c] & [e] \\ [e]^{\mathrm{T}} & -[\varepsilon] \end{bmatrix} \begin{Bmatrix} \{S\} \\ -\{E\} \end{Bmatrix}, \tag{35}$$

where $\{T\}$ is the stress vector of elastic substrate, $\{D\}$ the electric flux density vector, $\{S\}$ the strain vector of elastic substrate, $\{E\}$ the electric field vector, $\{c\}$ the elasticity matrix (evaluated at constant electric field), $[e]$ the piezoelctric matrix and $[\varepsilon]$ is the dielectric matrix (evaluated at constant mechanical strain).

The continuum model is discretized to produce a finite element model with nodal response variables and element shape functions over an element region that approximates the exact solution

$$\{u_c\} = [N^u]^{\mathrm{T}}\{u\}, \tag{36}$$

$$V_c = \{N^V\}^{\mathrm{T}}\{V\}, \tag{37}$$

in which $\{u_c\}$ is the element displacement vector in the local co-ordinate system, V_c the element electric potential, $[N^u]$ the matrix of displacement shape function, $\{N^V\}$ the vector of electric potential shape function and $\{u\}$ is the nodal displacement vector in the global co-ordinate system.

Strain and electric field are related to displacements and potentials, respectively as follows

$$\{S\} = [B_u]\{u\}, \{\{E\}\} = -[B_v][V], \quad \text{where } [B_u] = \begin{pmatrix} \frac{\partial}{\partial x} & 0 & 0 \\ 0 & \frac{\partial}{\partial y} & 0 \\ 0 & 0 & \frac{\partial}{\partial z} \\ \frac{\partial}{\partial y} & \frac{\partial}{\partial x} & 0 \\ 0 & \frac{\partial}{\partial z} & \frac{\partial}{\partial y} \\ \frac{\partial}{\partial z} & 0 & \frac{\partial}{\partial x} \end{pmatrix} [N^u]^{\mathrm{T}}, \quad [B_v] = \begin{pmatrix} \partial/\partial x \\ \partial/\partial y \\ \partial/\partial z \end{pmatrix} [N^V]^{\mathrm{T}}.$$

The finite element matrix equation of the coupled system in global co-ordinates is expressed

$$\begin{bmatrix} [M] & [0] \\ [0] & [0] \end{bmatrix} \begin{Bmatrix} \{\ddot{u}\} \\ \{\ddot{V}\} \end{Bmatrix} + \begin{bmatrix} [C] & [0] \\ [0] & [0] \end{bmatrix} \begin{Bmatrix} \{\dot{u}\} \\ \{\dot{V}\} \end{Bmatrix} + \begin{bmatrix} [K] & [K^z] \\ [K^z]^{\mathrm{T}} & [K^d] \end{bmatrix} \begin{Bmatrix} \{u\} \\ \{V\} \end{Bmatrix} = \begin{Bmatrix} \{F\} \\ \{L\} \end{Bmatrix}, \tag{38}$$

where $[M]$ = structural mass matrix $= \iint \int_{vol} \rho_s [N^u][N^u]^{\mathrm{T}} \, \mathrm{d}(vol)$, $[C]$ = structural damping matrix, $[K]$ = structural stifness matrix $= \iint \int_{vol} [B_u]^{\mathrm{T}}[c][B_u] \, \mathrm{d}(vol)$, $[K^d]$ = dielectric conductivity matrix $= \iint \int_{vol} [B_v]^{\mathrm{T}}[\varepsilon][B_v] \, \mathrm{d}(vol)$, $[K^z]$ = piezoelectric couplig matrix $= \iint \int_{vol} [B_u]^{\mathrm{T}}[e][B_u] \, \mathrm{d}(vol)$, $\{F\}$ = structural load vector (vector of nodal forces, suface forces and body forces), and $\{L\}$ = electric load vector, applied nodal charge vector.

The finite element *structural* equation and the *fluid* wave equation are to be considered simultaneously in fluid–structure interaction problems. Introducing the notations for the gradient and divergence

$$\nabla \Phi = \{L\}\Phi, \tag{39}$$

$$\nabla \cdot \vec{F} = \{L\}^{\mathrm{T}}\vec{F} = \left\{\frac{\partial}{\partial x}\frac{\partial}{\partial y}\frac{\partial}{\partial z}\right\}\vec{F}, \tag{40}$$

one can rewrite the governing equation for the fluid wave equation as

$$\frac{1}{c^2}\frac{\partial^2 p}{\partial t^2} - \{L\}^{\mathrm{T}}\{L\}P = 0. \tag{41}$$

Given standard linear acoustic assumptions, fluid momentum equations yield the following relations between the normal pressure gradient of the fluid and the normal acceleration of the structure at a fluid–structure interface S [26]

$$\{n\}\{\nabla P\} = -\rho_0\{n\}\frac{\partial^2\{U\}}{\partial t^2} \quad \text{or} \quad \{n\}^{\mathrm{T}}(\{L\}P) = -\rho_0\{n\}^{\mathrm{T}}\left(\frac{\partial^2\{U\}}{\partial t^2}\right), \tag{42}$$

where $\{U\}^{\mathrm{T}} = \{uvw\}$ is the global displacement vector of the structure at the fluid/structure interface. The finite element approximating shape functions for the spatial variation of the pressure and displacement components are

$$P = \{N\}^{\mathrm{T}}\{P_e\}, \quad \{U\} = \begin{Bmatrix} u \\ v \\ w \end{Bmatrix} = \begin{Bmatrix} \{N'\}^{\mathrm{T}}\{u_e\} \\ \{N'\}^{\mathrm{T}}\{v_e\} \\ \{N'\}^{\mathrm{T}}\{w_e\} \end{Bmatrix} = \{N'\}^{\mathrm{T}}\{U_e\}, \tag{43}$$

with $\{N\}$ the element shape function for pressure, $\{N'\}$ the element shape function for displacement, $\{P_e\}$ the nodal pressure vector in element co-ordinates, $\{U_e\}$ the nodal displacement component vectors in element co-ordinates and $\{U\}$ is the structural nodal displacement vector in global co-ordinates.

From the above relations, one can write a Galerkin variational form for the wave equation

$$\int\int\int_{vol}\frac{1}{c^2}\{\delta P_e\}^{\mathrm{T}}\{N\}\{N\}^{\mathrm{T}}\,\mathrm{d}(vol)\{\ddot{P}_e\} + \int\int\int_{vol}\{\delta P_e\}^{\mathrm{T}}[B]^{\mathrm{T}}[B]\,\mathrm{d}(vol)\{P_e\} + \int\int_S \rho_0\{\delta P_e\}^{\mathrm{T}}\{N\}\{n\}^{\mathrm{T}}\{N'\}^{\mathrm{T}}\,\mathrm{d}S\{\ddot{U}\} = 0, \tag{44}$$

where $\{n\}$ is the normal to the surface S at the fluid boundary. In terms of finite elements, this variational equation transforms into the matrix equation

$$[M_e^p]\{\ddot{P}_e\} + [K_e^p]\{P_e\} + \rho_0[R_e]^{\mathrm{T}}\{\ddot{U}\} = \{0\}, \tag{45}$$

with

$$[M_e^p] = \text{fluid mass matrix} = \frac{1}{c^2}\int\int\int_{vol} \{N\}\{N\}^{\mathrm{T}}\,\mathrm{d}(vol),$$

$$[K_e^p] = \text{fluid stiffness matrix} = \int\int\int_{vol} [B]^{\mathrm{T}}[B]\,\mathrm{d}(vol),$$

$$\rho_0[R_e] = \text{coupled mass matrix} = \rho_0\int\int_S \{N\}\{n\}^{\mathrm{T}}\{N'\}^{\mathrm{T}}\,\mathrm{d}S.$$

In order to account for the dissipation of energy due to radiation at the truncated fluid domain boundary, a second surface integral term is incorporated into the wave equation as a dissipation term [27]

$$[C_e^p]\{\dot{P}_e\} = \frac{\beta}{c_f}\int\int_{S_B} \{N\}\{N\}^{\mathrm{T}}\,\mathrm{d}s\{\dot{P}_e\}. \tag{46}$$

If $\beta = c_f$, the addition of the above surface integral into the fluid wave equation is essentially equivalent to applying a first order Sommerfeld radiation condition. ($[C_e^P]$ is referred to as the damping matrix).

Combining all terms for the fluid, the finite element matrix equation governing the acoustic fluid is

$$[M_e^p]\{\ddot{P}_e\} + [C_e^p]\{\dot{P}_e\} + [K_e^p]\{P_e\} + \rho_0[R_e]^{\mathrm{T}}\{\ddot{U}\} = \{0\}. \tag{47}$$

For the coupled fluid–structure interaction problem, the fluid pressure load acting at the interface is added to the structure equation of motion as follows

$$[M_e]\{\ddot{U}_e\} + [C_e]\{\dot{U}_e\} + [K_e]\{U_e\} = \{F_e\} + \{F_e^{pr}\}, \tag{48}$$

where $\{M_e\}$ is the global structural mass matrix, $\{C_e\}$ the global structural damping matrix, $\{K_e\}$ the global structural stiffness matrix, $\{U_e\}$ the nodal displacement vectors in global co-ordinates, $\{F_e\}$ the nodal load vector and $\{F_e^{pr}\}$ is the fluid pressure load vector.

The fluid pressure load vector at the interface S is obtained by integrating the pressure

$$\{F_e^{pr}\} = \int\int_S \{N'\}\{N\}^{\mathrm{T}}\{n\}\,\mathrm{d}S\{P_e\} = [R_e]^{\mathrm{T}}\{P_e\}, \tag{49}$$

where $[R_e]$ is the transpose of the coupled mass matrix. Substitution of the above expression into the coupled fluid–structure equation of motion

$$[M_e]\{\ddot{U}_e\} + [C_e]\{\dot{U}_e\} + [K_e]\{U_e\} - [R_e]\{P_e\} = \{F_e\}. \tag{50}$$

This matrix equation combined with the finite element form of the fluid wave equation that includes fluid and damping elements becomes the system

$$\begin{bmatrix} [M_e] & [0] \\ [M^{fs}] & [M_e^p] \end{bmatrix}\begin{Bmatrix} \{\ddot{U}_e\} \\ \{\ddot{P}_e\} \end{Bmatrix} + \begin{bmatrix} [C_e] & [0] \\ [0] & [C_e^p] \end{bmatrix}\begin{Bmatrix} \{\dot{U}_e\} \\ \{\dot{P}_e\} \end{Bmatrix} + \begin{bmatrix} [K_e] & [K^{fs}] \\ [0] & [K_e^p] \end{bmatrix}\begin{Bmatrix} \{U_e\} \\ \{P_e\} \end{Bmatrix} = \begin{Bmatrix} \{F_e\} \\ \{0\} \end{Bmatrix}, \tag{51}$$

where

$$[M^{fs}] = \rho_0[R_e]^{\mathrm{T}} \quad \text{and} \quad [K^{fs}] = -[R_e].$$

For a problem involving fluid–structure interaction, the acoustic fluid element formulation generates all the sub-matrices with superscript p in addition to the coupling sub-matrices. Subscripts without a superscript are generated by the compatible structural element used in the model. The system is solved to determine all dependent variables including fluid pressure, voltage potentials, and displacements.

5.2. Finite difference/boundary integral methods

Applying a Green's function argument, the scattered pressure degrees of freedom at the surface of the fluid/solid interface can be eliminated. The fluid pressure at the interface is then replaced by a continuum of point sources (Green's functions) weighted by the normal acceleration of the elastic plate. With the normal acceleration of the plate found, the scattered pressure is easily found by a boundary integral expression involving Green's function. The derivation of the integral equation is as follows.

The two-dimensional half-space Green's function is found using the free space Green's function and the method of images. It is given by [28]

$$G(x,\xi,z,\eta) = -\frac{\mathrm{i}}{4}\left\{H_0^1(k_f\sqrt{(x-\xi)^2+(z-\eta)^2}) + H_0^1(k_f\sqrt{(x-\xi)^2+(z+\eta)^2})\right\}, \tag{52}$$

where (ξ,η) are the co-ordinates of the line source, and (x,z) are co-ordinates of the field point. One can use Green's function to represent the fluid pressure at the fluid solid interface by an integral involving the normal derivative of the scattered fluid pressure

$$\int_0^L G(x,\xi,0,\eta)\frac{\partial p_S}{\partial z}(x,0)\,\mathrm{d}x = \begin{cases} 0 & \text{if } \eta<0, \\ \frac{1}{2}p_s(\xi,\eta) & \text{if } \eta=0, \\ p_s(\xi,\eta) & \text{if } \eta>0, \end{cases} \tag{53}$$

that upon substitution of the normal acceleration in lieu of the value of the normal derivative of the pressure at the fluid/solid interface (by Euler's equation), yields:

$$\frac{-\mathrm{i}\omega^2\rho_f}{2}\int_0^L H_0(k_f\sqrt{(x-\xi)^2+\eta^2})w(x,0)\,\mathrm{d}x = \begin{cases} 0 & \text{if } \eta<0, \\ \frac{1}{2}p_s(\xi,\eta) & \text{if } \eta=0, \\ p_s(\xi,\eta) & \text{if } \eta>0. \end{cases} \tag{54}$$

Switching the variables $(\xi,\eta)\Leftrightarrow(x,z)$, the integral can be used to replace the scattered pressure expression in the normal stress boundary condition at the fluid/solid interface (at $z=0$), leading to the interface conditions:

$$(\lambda+2\mu)\frac{\partial w_e}{\partial z} + \lambda\frac{\partial u_e}{\partial x} = \mathrm{i}\omega^2\rho_f\int_0^L H_0(k_f|x-\xi|)w(\xi,0)\,\mathrm{d}\xi - (p_I+p_R), \tag{55}$$

$$\mu\left(\frac{\partial w_e}{\partial x}+\frac{\partial u_e}{\partial z}\right) = 0. \tag{56}$$

Matrix equations result from discretizing the equations of motion and boundary or interface conditions, leading to a system of equations. The degrees of freedom include the horizontal and vertical displacements at each node for elastic, viscoelastic and piezoelectric materials, as well as a degree of freedom at each node in the piezoelectric material for the electric potential.

A second order finite difference scheme is employed for the governing equations at all interior nodes. At free surfaces or fluid solid interfaces, a third order Taylor series approximation is adopted. Essentially, the value of a dependent variable at an interior node is expanded in terms of its value at the surface, its normal derivative at the surface (taken from the boundary conditions), and its second normal derivative at the surface (in which the governing equation is used). At an interface between elastic and piezoelectric or viscoelastic materials, an averaged expression involving Taylor series is used to satisfy continuity boundary conditions [29]. This formulation has the nice feature that when the two elastic materials in contact have identical material properties, the interface differencing reverts to the standard second order differencing template for an interior point of the elastic material.

For the integral expression, a second order accurate trapezoidal rule of integration is used except at points where the integrand has a logarithmic singularity. At these points, the asymptotic form for the Hankel function for small argument is used, and the integration is done analytically. The discrete form of the integral expression evaluated at the surface point $x = x_i$ is given by

$$\mathrm{i}\omega^2\rho_f\Delta x\sum_{\substack{l=2\\ l\neq i}}^{50} H_0(k_f|x_i - x_l|)w(x_l,0) - \frac{2\omega^2\rho_f\Delta x}{\pi}w(x_i,0)\left[\ln\left(\frac{k_f\Delta x}{2}\right) - 1\right]. \tag{57}$$

Gaussian elimination with partial pivoting is used to solve the resulting system of equations. The stated problem is forced by either: an applied voltage across the piezoelectric layer, an incident pressure coming from the fluid, or a combination of the two. The pressure at arbitrary field points in the fluid are found by again applying a boundary integral method which essentially weights the fluid half-space Greens' function by accelerations at the surface of the fluid/solid interface.

6. Results and discussion

For the first problem, there is an infinite fluid loaded bilaminate plate, with upper layer composed of steel and a lower layer composed of a viscoelastic material. Each layer has thickness 1 cm, and on the vacuum side of the bilaminate, there is applied a normal pressure or a 60° phased pressure of amplitude 1 Pa operating at a range of frequencies. The solutions plotted are found by employing the invariant embedding technique. To analyze the effectiveness of the viscoelastic layer in reducing unwanted radiated acoustic energy, pressure amplitudes are also given at each frequency for radiation from a 1 cm, fluid loaded, steel plate (i.e., the bilaminate without the viscoelastic layer).

Fig. 3 shows that the viscoelastic layer does little to reduce the amount of radiated acoustic energy for the bilaminate. For the zero degree phasing of the applied pressure, the amplitude of the radiated pressure is in fact greater than that for the elastic layer alone for frequencies above about 14 kHz.

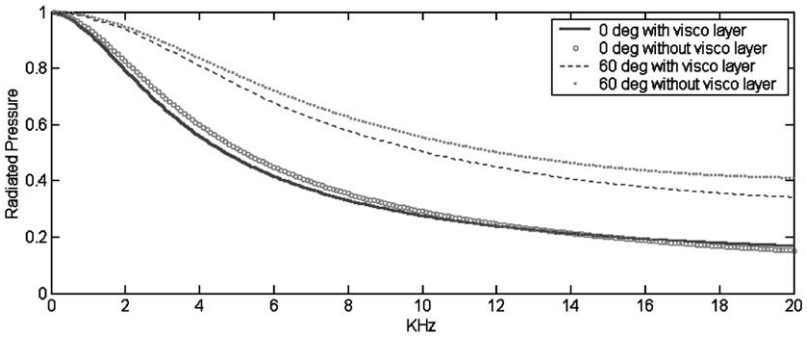

Fig. 3. Radiated pressure with and without viscoelastic layer of 1 cm thickness steel, applied pressure = 1 Pa.

The invariant embedding technique has been tested by comparing with the potential method, described in Eqs. (31)–(34), for the case of plane wave radiation from an infinite fluid loaded layer. Pressure radiation from a single infinite layer of 1 cm plate of elastic or viscoelastic material for the incident pressure of 0° and 60° phase is shown in Fig. 4 which displays the exact match between the invariant embedding method and potential method.

An alternative strategy would be to sandwich the viscoelastic layer between two elastic layers of equal thickness. In Fig. 5, radiation from a 1 cm viscoelastic layer sandwiched between two 0.5 cm steel layers is compared with radiation from a single 1 cm layer of steel. For the unphased pressure, the results are similar to the bilaminate result until frequencies of about 6 kHz, at which frequency the viscotrilaminate is less effective in suppressing the radiated pressure. When the applied pressure is phased by 60°, the differences between the purely elastic layer and trilaminate are more pronounced. Note that at about 3 kHz, there is a dramatic drop in the radiated pressure amplitude due to absorption of energy by the viscoelastic layer.

A finite bilaminate is more physically realizable, but embedding methods can no longer be employed. In such a case, one must resort to numerical methods such as finite difference or finite element techniques. The next series of graphs will refer to a bilaminate plate of length 0.25 m with steel (thickness 1 cm) and PZT4 (thickness 2 cm), which is held fixed in an acoustically hard baffle of infinite extent. Comparisons are made between a finite difference code and the finite element code ANSYS for the purpose of benchmarking.

In the first example, a pure radiation problem is considered. At 1000 Hz, a 1 V (real and imaginary) potential is set across the PZT4 layer, and the radiated pressure in the fluid is determined. The bilaminate plate is considered to be simply supported. In Figs. 6–8, the pressure amplitude at a series of points in the fluid normal to the bilaminate, followed by the amplitude of the pressure measured at 1 m from the center of the bilaminate, and finally the amplitude of the normal surface displacement of the bilaminate, is displayed for both FEM and FDM. The results appear to match well. FEM pressure contour of the field due to the voltage in piezoelectric layer is presented in Fig. 9.

A second problem using the same physical set-up analyzes the results of point source scattering from the baffled bilaminate. A line source of amplitude $A_p = 40$, is placed about $\frac{1}{2}$ meter above the center of the plate, and the total pressure is found in the fluid. The total pressure is given since the scattered pressure has a magnitude much less than the incident and specularly reflected pressures.

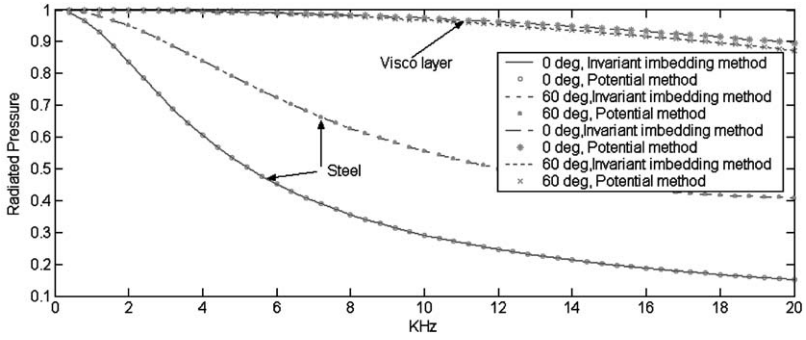

Fig. 4. Radiated pressure from 1 cm of elastic or viscoelastic layer, applied pressure = 1 Pa.

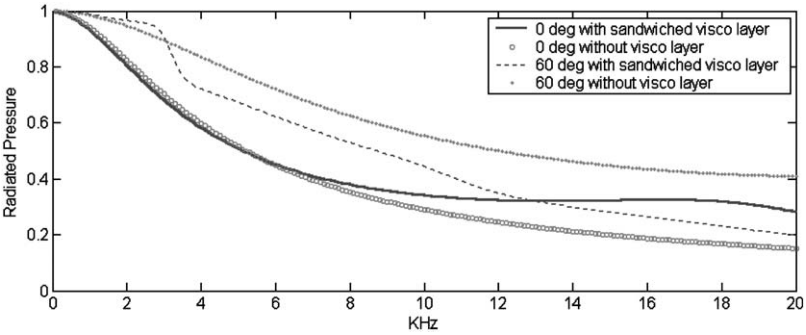

Fig. 5. Radiated pressure with and without sandwiched viscoelastic layer for the case of 1 cm thick steel, with and without 1 cm thick visco layer, applied pressure = 1 Pa.

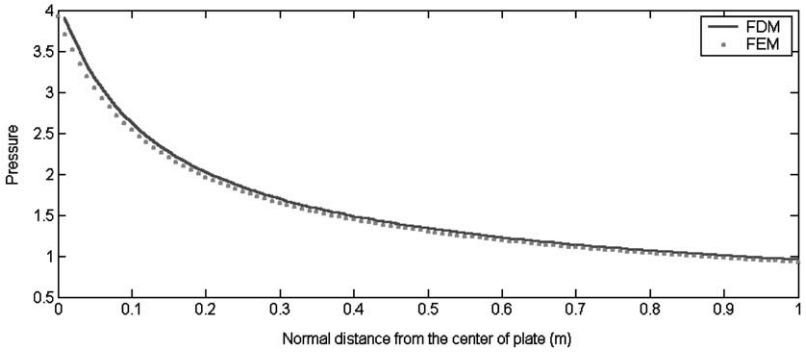

Fig. 6. Pressure along the line normal to the center of plate (baffled 0.25 bilaminate, 10 mm steel, 20 mm PZT4) subjected to voltage of 1 V (real and imaginary) at frequency of 1000 Hz.

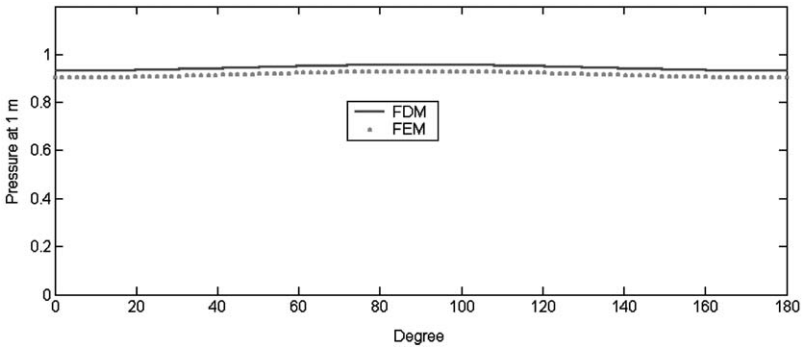

Fig. 7. Pressure along the radial boundary of radius 1 m (baffled 0.25 bilaminate, 10 mm steel, 20 mm PZT4) subjected to voltage of 1 V (real and imaginary) at frequency of 1000 Hz.

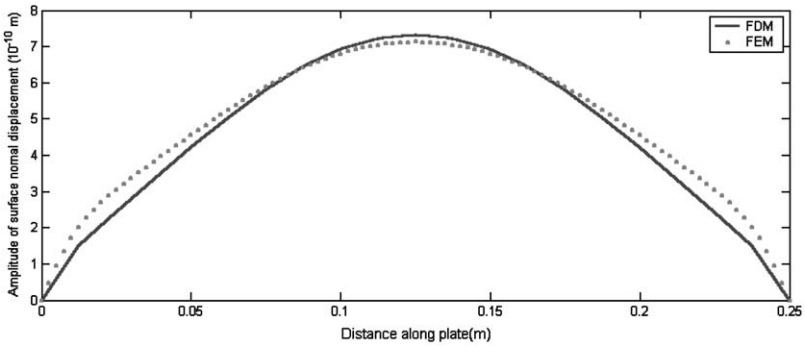

Fig. 8. Amplitude of vertical displacement along the top surface of elastic substrate (baffled 0.25 bilaminate, 10 mm steel, 20 mm PZT4) subjected to voltage of 1 V (real and imaginary) at frequency of 1000 Hz.

(The specularly reflected pressure is due to the acoustically hard baffle). Calculation of the scattered pressure is possible in the FDM code since the incident *plus* specularly reflected pressures are used as inputs to determine the scattered pressure due to the presence of the bilaminate. With the scattered pressure found from the FDM code, the total pressure is easily calculated by adding in the incident and specularly reflected pressures. In the FEM code, all pressure fields are combined, and it is a difficult matter to extract the scattered pressure, which is of small amplitude relative to the incident and specularly reflected pressures.

In comparing the FDM and FEM results, Figs. 10 and 11 are shown. In each case, the voltage potential across the PZT4 is zero; therefore this may be considered a pure scattering problem. Fig. 10 gives the amplitude of the pressure along a centered, normal line from the baffled plate. Fig. 11 plots the amplitude of the pressure, at 1 m from the center point of the plate, as a function of angle from the plate surface. Comparisons between the FEM and FDM codes are quite good.

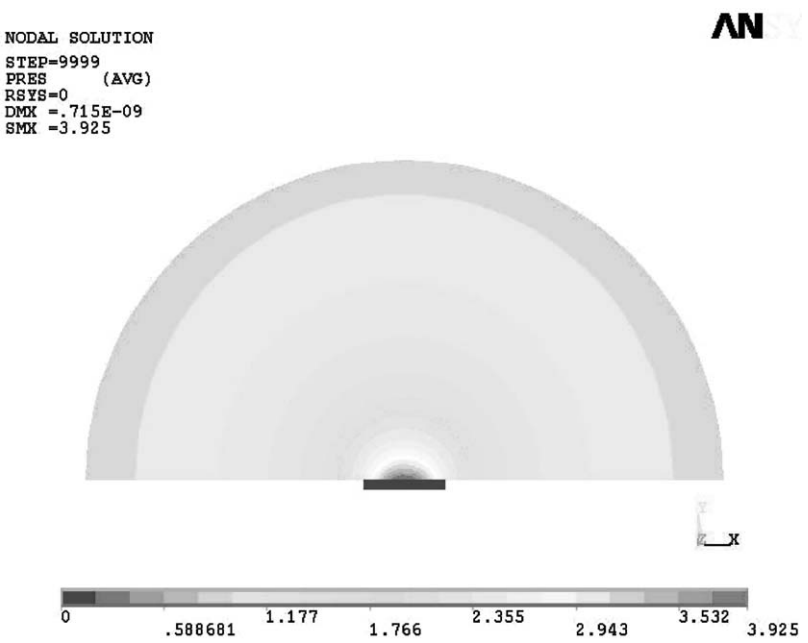

Fig. 9. Radiated pressure by the active piezoelectric element (baffled 0.25 bilaminate, 10 mm steel, 20 mm PZT4) subjected to voltage of 1 V (real and imaginary) at frequency of 1000.

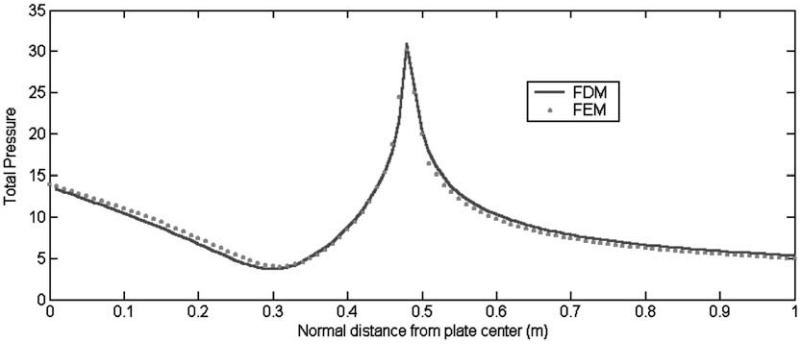

Fig. 10. Pressure along the line normal to center of plate for the case of scattering (baffled 0.25 bilaminate, 10 mm steel, 20 mm PZT4) due to flow source of strength 40 kg/s^2 at frequency of 1000, where piezo is short circuited.

From the solutions to the previous two cases, it is possible to calculate an applied voltage potential that has the effect of canceling either the total or scattered pressure at any point in the fluid caused by the scattering or reflection of the incident line source. In particular, if the point chosen is at 1 m directly above the centerline of the plate, a voltage is found by scaling the radiated

pressure at 1 m with a 1 V potential difference by the total (or scattered) pressure calculated from the pure scattering problem at 1 m. Figs. 12 and 13 show both the finite difference and finite element results of performing this step as a combined scattering/radiation problem to cancel the total pressure at 1 m. FEM pressure contours are presented in Figs. 14 and 15 for the case of before and after control of the total pressure in the point of interest.

If only the scattered pressure is to be cancelled, the piezoelectric layer is much more effective. Fig. 16 employs a voltage difference that cancels the scattered pressure at 1 m using the finite difference method. The amplitudes of the pressures at 1 meter from the plate center are displayed in term of dB re 1 μPa. Note that for the full range of angles, there is more than a 40-point drop of the scattered pressure amplitude when the voltage is applied.

Cancellation of one field point using active piezoelectric element has been described in this paper. Global and local acoustics field reduction can be achieved using multiple piezoelectric elements with different voltages applied for different piezoelectric elements. Both viscoelastic

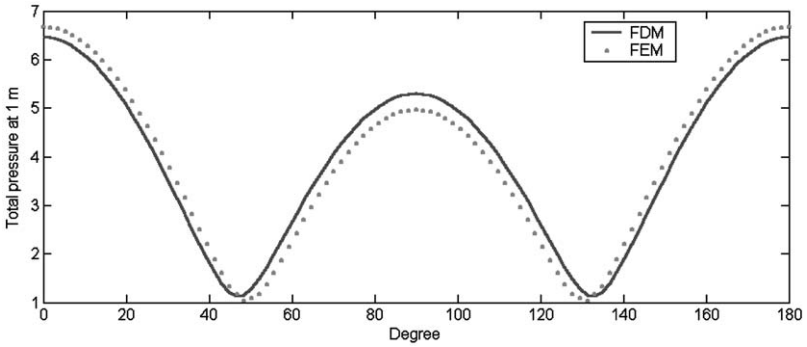

Fig. 11. Pressure along the radial boundary of radius 1 m for the case of scattering (baffled 0.25 bilaminate, 10 mm steel, 20 mm PZT4) due to flow source of strength 40 kg/s^2 at frequency of 1000, where piezo is short circuited.

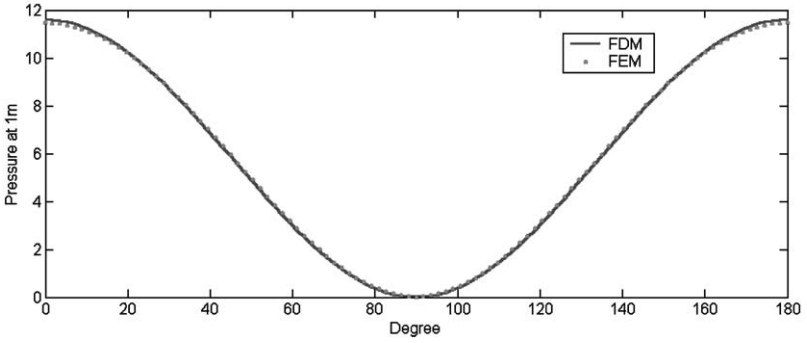

Fig. 12. Pressure along the radial boundary of radius 1 m for the case of for the case of radiation and scattering (baffled 0.25 bilaminate, 10 mm steel, 20 mm PZT4, flow source of strength 40 kg/s^2) at frequency of 1000, voltage of 7.564(-8.7445°) applied in the piezo.

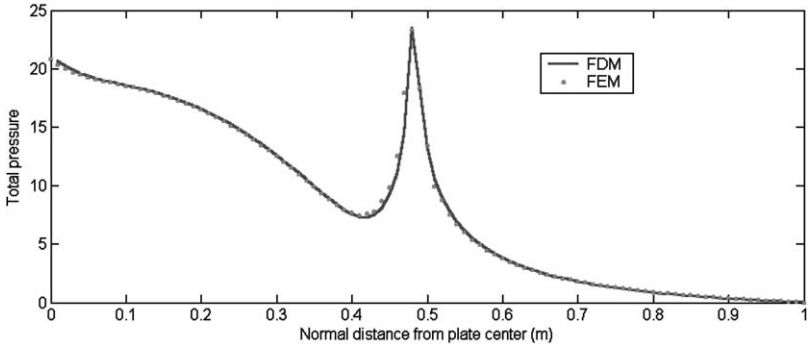

Fig. 13. Pressure along the line normal to center of plate for the case of for the case of radiation and scattering (baffled 0.25 bilaminate, 10 mm steel, 20 mm PZT4, flow source of strength 40 kg/s^2) at frequency of 1000, voltage of 7.564(−8.74450) applied in the piezo.

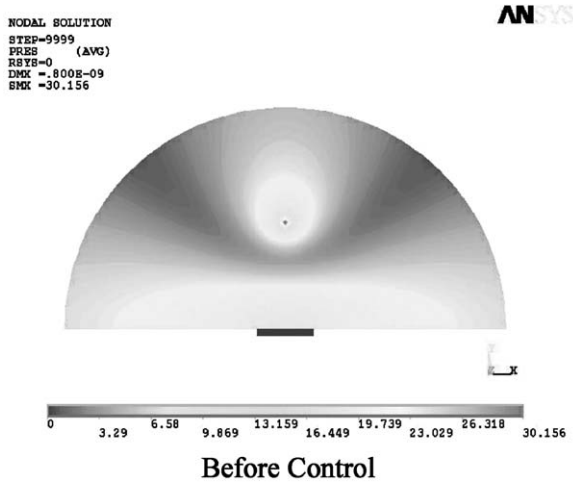

Fig. 14. Contour of pressure for the case of scattering (baffled 0.25 bilaminate, 10 mm steel, 20 mm PZT4) due to flow source of strength 40 kg/s^2 at frequency of 1000, where piezo is short circuited.

material and piezoelectric material can be used together for the hybrid active/passive control of acoustic signature where optimization technique will be used for the selection of number, size and location of the material depending on the control objective.

7. Conclusion

In order to develop the analytical treatment and mathematical formulation for predicting the acoustic performance of both viscoelastic and piezoelectric material embedded on a fluid-loaded plate, cancellation technique of scattered or radiated acoustics signals using piezoelectric and

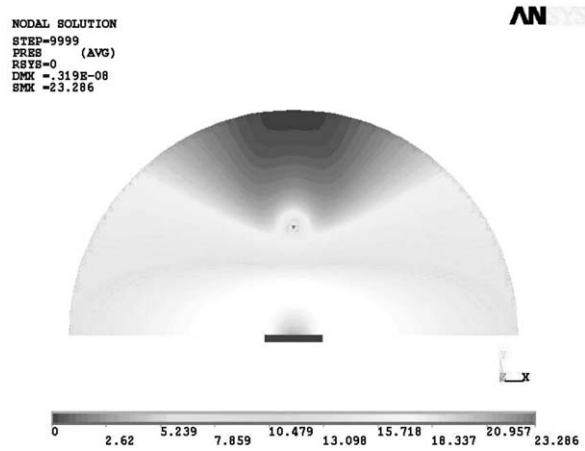

Fig. 15. Contour of pressure for the case of for the case of radiation and scattering (baffled 0.25 bilaminate, 10 mm steel, 20 mm PZT4, flow source of strength 40 kg/s^2) at frequency of 1000, voltage of 7.564(-8.7445°) applied in the piezo.

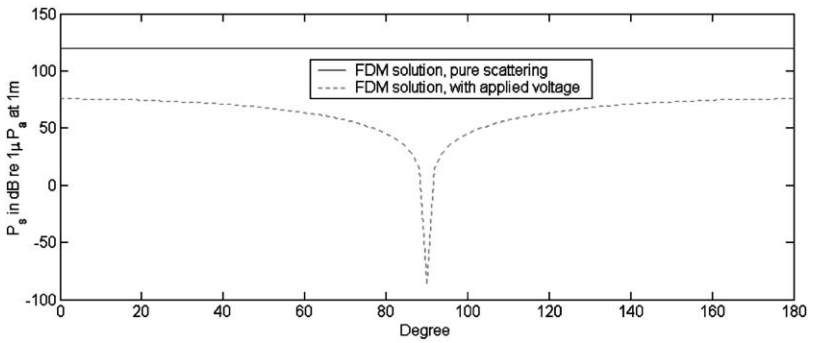

Fig. 16. Pressure along the radial boundary of radius 1 m for the case of only scattered pressure reduction (baffled 0.25 bilaminate, 10 mm steel, 20 mm PZT4, flow source of strength 40 kg/s^2) at frequency of 1000.

viscoelastic material has been implemented. Invariant embedding technique describing the viscoelastic property of the bilaminate has been verified with a simple potential method. It can be concluded that the use of viscoelastic layers alone in efforts to reduce unwanted acoustic radiation is not particularly effective. Use of viscoelastic layer to reduce scattered pressures is even less effective. Acoustic signal reduction using piezoelectric and viscoelastic material in both FEM and FDM has been described. FEM results by ANSYS code are in good agreement with that of FDM analysis. The mathematical formulation presented in this paper provides a guide for future use of hybrid active/passive control of sound radiation/scattering. Work needs be done in modelling more complicated structures, as well as constructing control mechanisms capable of reducing

backscatter. Three-dimensional FEM modelling and experiment for underwater acoustic signal reduction are for future study.

References

[1] A.J. Tucker, Division of Ship Structures and Systems Science and Technology, Ship & Submarine Signature Research, Office of Naval Research "home page", April 1997.
[2] G.R. Tomlinson, An overview of active/passive damping techniques employing visocoelastic materials, in: P.F. Gobin, J. Tatibouët (Eds.), *Third International Conference on Intelligent Materials*, Lyon, France, 3–5 June 1996.
[3] G.A. Brigham, J. Libuha, R.P. Radlinski, Analysis of scattering from large planar gratings of compliant cylindrical shells, *Journal of the Acoustical Society of America* 61 (1977) 48–59.
[4] G. Gaunaurd, One-dimensional model of acoustic absorption in a viscoelastic medium containing short cylindrical cavities, *Journal of the Acoustical Society of America* 62 (1977) 298–307.
[5] R. Lane, Absorption mechanisms for waterborne sound in Alberich anechoic layers, *Ultrasonics* 18 (1981) 28–30.
[6] Toulis, Acoustic refraction and scattering with compliant elements, *Journal of the Acoustical Society of America* 29 (1957) 1021–1033.
[7] R.P. Radlinski, Scattering from multiple gratings of compliant tubes in a viscoelastic layer, *Journal of the Acoustical Society of America* 85 (1989) 2301–2310.
[8] A. DiMeglio, J.C. Jones, R.F.W. Coates, D.T.I. Francis, L.S. Wang, Combined finite element-boundary element analysis of a viscoelastic anechoic panel for underwater applications, *Oceans '97, MTS/IEEE Conference Proceedings*, October 1997, Halifax, Canada, pp. 1189–1194.
[9] O.B. Wilson, *Introduction to Theory and Design of Sonar Transducers*, Peninsula Publishing Co, Los Altos, CA, 1988.
[10] X.Q. Bao, V. Varadan, V. Varadan, T.R. Howarth, Model of a bilaminar actuator for active acoustic control systems, *Journal of the Acoustical Society of America* 87 (1990) 1350–1352.
[11] A.M.B. Braga, Suppression of sound reflected from a piezoelectric plate, *Journal of Intelligent Material Systems and Structures* 3 (1992) 209–223.
[12] T.R. Howarth, V. Varadan, X. Bao, V. Varadan, Piezocomposite coating for active underwater sound reduction, *Journal of the Acoustical Society of America* 91 (1992) 823–831.
[13] J. Kim, V. Varadan, V. Varadan, Modeling integrated sensor/actuator functions in realistic environments, *Smart Structures and Materials, SPIE Proceedings*, Vol. 1916, 1993, pp. 56–64.
[14] J. Kim, V. Varadan, V. Varadan, Finite element modeling of a finite piezoelectric sensor/actuator embedded in a fluid-loaded plate, *Mathematics and Control in Smart Structures, SPIE Proceedings*, Vol. 2192, 1994, pp. 273–280.
[15] L.D. Lafleur, F.D. Shields, Hendrix acoustically active surfaces using piezorubber, *Journal of the Acoustical Society of America* 90 (1991) 1230–1237.
[16] F.B. Jensen, W.A. Kuperman, M.B. Porter, H. Schmidt, *Computational Ocean Acoustics*, AIP Press, New York, 1994.
[17] ANSYS, Element Reference, Release 5.4, ANSYS, Inc., September 1997.
[18] A.D. Nashif, D.I.G. Jones, J.P. Henderson, *Vibration Damping*, Wiley, New York, NY, 1985.
[19] A.M. Baird, F.H. Kerr, D.J. Townend, Wave propagation in a viscoelastic medium containing fluid-filled miscrospheres, *Journal of the Acoustical Society of America* 105 (1999) 1527–1537.
[20] J.D. Achenbach, *Wave Propagation in Elastic Solids*, North-Holland, New York, 1980.
[21] B.A. Auld, *Acoustic Fields and Waves in Solids*, Vol. I, Krieger Publishing Co, Malabar, FL, 1990.
[22] K. Aki, P.G. Richards, *Quantitative Seismology, Theory and Methods*, W.H. Freeman and Co., New York, 1980.
[23] B. Honein, A.M.B. Braga, P. Barbone, G. Herrmann, Wave propagation in piezoelectric layered media with some applications, *Journal of Intelligent Material Systems and Structures* 2 (1991) 542–557.
[24] J.D. Achenbach, *Wave Propagation in Elastic Solids*, North-Holland, New York, 1980.

[25] ANSYS, Theory Reference, Release 5.4, ANSYS, Inc., Sept. 1997.
[26] O.C. Zienkiewicz, R.E. Newton, Coupled vibrations of a structure submerged in a compressible fluid, *Proceedings of the Symposium on Finite Element Techniques*, University of Stuttgart, Germany, June 1969.
[27] A. Craggs, Finite element model for acoustically lined small rooms, *Journal of Sound and Vibration* 108 (2) (1986) 327–337.
[28] M.C. Junger, D. Feit, *Sound, Structures, and their Interaction*, MIT Press, Cambridge, MA, 1986.
[29] C.L. Scandrett, J.D. Achenbach, Time domain finite difference calculations for interaction of an ultrasonic wave with a surface breaking crack, *Wave Motion* 9 (1987) 171–190.